Metals Materials And Processes, 2000, Vol. 12, No. 2 & 3, pp. 161 - 180.

SYNTHESIS, PROCESSING, SINTERING AND CHARACTERISATION OF SPECIAL CERAMIC MATERIALS

T. S. Kannan, P. K. Panda, V. A. Jaleel, R. Ramachandra Rao, H. N. Roopa,
L. Mariappan and A. Cheluvaraju,
Materials Science Division, National Aerospace Laboratories, Bangalore 560 012, India.

(Received 10 January 2000)

Abstract : Hydrothermal and carbothermal synthesis as specific material synthesis routes to obtain simple oxide powders (e.g. acicular ferromagnetic chromium dioxide and alumina in fine powder form) as well as composite oxide powders (e.g. alumina and zirconia) containing β-silicon carbide whiskers as a second phase toughener have been extensively investigated and some significant results are summarised. Ceramic processing followed by reaction nitridation of silicon, silicon + silicon carbide and silicon + silicon nitride powder mixtures in various ratios have been studied and some representative results are presented herein. Synthesis of hydroxyapatite powder and its characterisation is also reported. Mechanical characterisation of some of these products have been studied and these are presented. An ascending thermal shock cum thermal fatigue test equipment fabricated for testing ceramic materials under an ascending thermal shock or combined ascending + descending thermal fatigue cycle is described.

Keywords : ceramic material, composite oxide powders, synthesis, processing, characterization

1. INTRODUCTION

This article is a brief summary of some research activities carried out in the areas of ceramic material synthesis, characterisation and ceramic processing by the above team since the last one decade. One set of activities have been directed towards researches on material synthesis using solid state, hydrothermal and carbothermal reaction routes to produce monolithic and composite ceramic oxide powders (e.g. Calcium hydroxyapatite, CrO_2, α-Al_2O_3, Si_3N_4, Al_2O_3-SiC whisker (w), ZrO_2-SiC (w), Al_2O_3-ZrO_2-SiC (w) and Al_2O_3-sialon-SiC (w) etc. where w = whisker). Reaction nitridation of silicon powder as well as its mixtures with α-SiC particulates has been carried out to generate shaped composite specimens (in the form of bars, discs, cylinders etc.) of nitride bonded silicon carbide (NBSC; Si_3N_4 - SiC) and nitride bonded silicon nitride (NBSN; Si_3N_4 - Si_3N_4) using a high carbon activity graphite furnace.

Ceramic powder processing activities have centred on the development and characterisation of aqueous slurries containing a homogeneous dispersion of the ceramic particulates under high solid loading (e.g. Silicon, Silicon Carbide, Silicon nitride etc.). Such slurries or slips are suitable for generating slip cast bodies of various monolithic and composite ceramic materials of high green density. Powder pressing routes by uniaxial pressing in metallic dies have also been utilised for compacting composite powders generated by hydrothermal and carbothermal routes.

Consolidation (by sintering) of the various processed and shaped green ceramic bodies under various atmospheres e.g. under ambient atmosphere and ambient pressure, under a high carbon activity (in a graphite furnace), under an inert (argon) gas or reactive (nitrogen) gas pressure or under hot pressing in graphite dies at high temperature has been investigated.

Mechanical characterisation of the products has been carried out by measurement of their flexure strengths, fracture toughness and stiffness. Thermal characterisation in terms of rapid ascending thermal shock as well as of thermal fatigue behaviour on

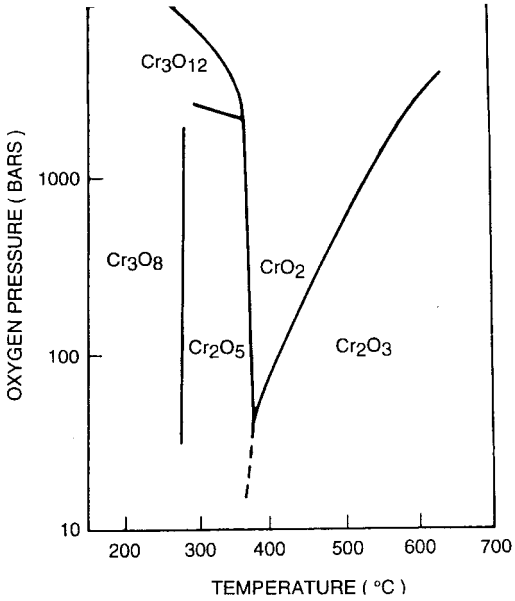

Fig. 1. The chromium - oxygen phase diagram

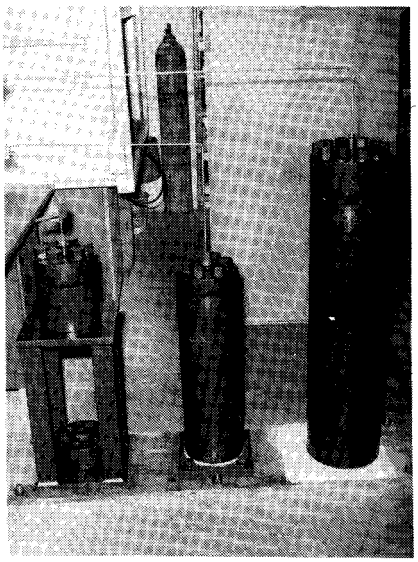

Fig. 2. Autoclaves used for the synthesis of (a) 100g (b) 1.5kg and (c) 5kg of CrO_2

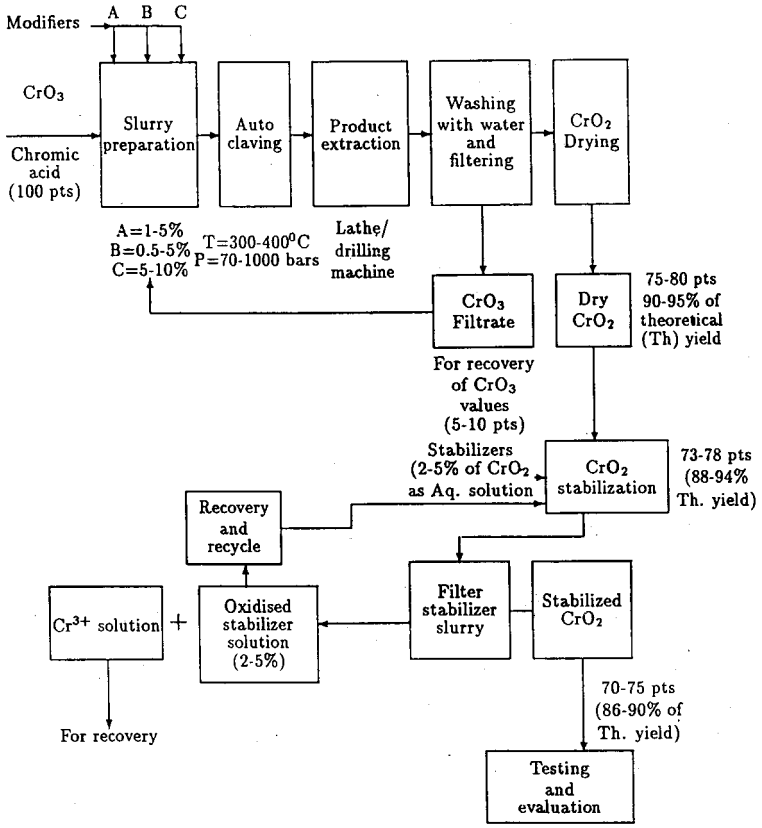

Fig. 3. Process flow sheet for preparation of acicular ferromagnetic chromium dioxide powders

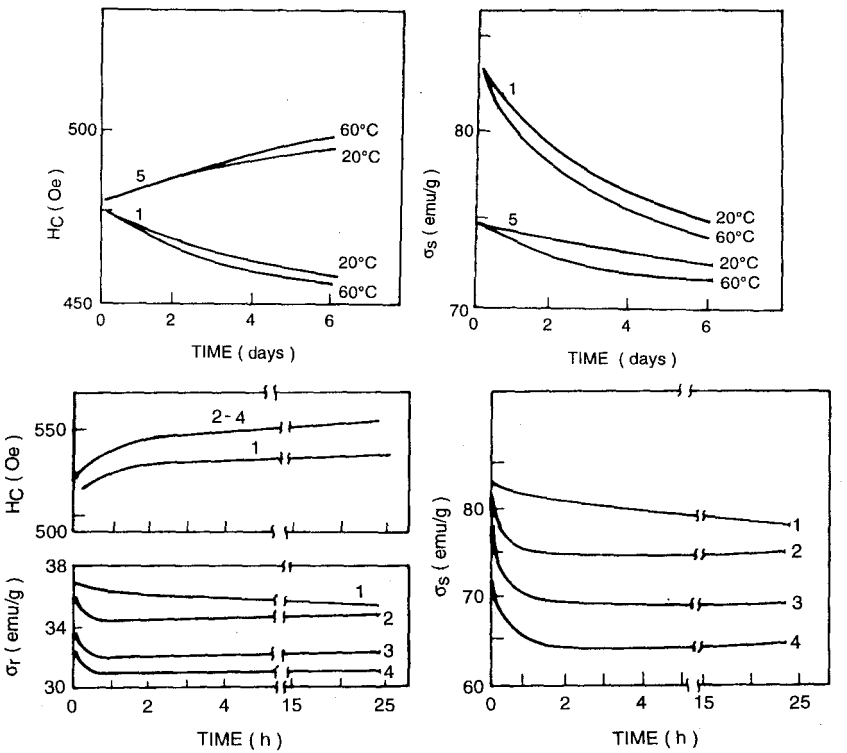

Fig. 4. Ageing behaviour of unstabilised and surface stabilised CrO_2 powders in water. Magnetic characteristics of CrO_2 powders as a function of the time of contact with stabilising solutions (SMBS) of different strengths: (1) unreacted (2) 3% aq. SMBS (3) 6% aq. SMBS (4) 10% aq. SMBS and (5) 15% aq. SMBS.

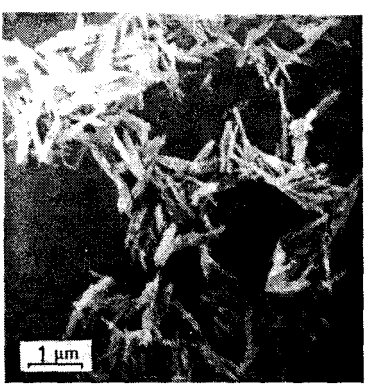

Fig. 5. SEM picture of typical CrO_2 powders.

specimens of the above ceramic materials could now be carried on a special equipment developed recently for the purpose. Some results generated using this novel equipment are presented.

2. HYDROTHERMAL SYNTHESIS OF CERAMIC MATERIALS

Hydrothermal synthesis of materials has had a long history at NAL dating back to 1975 when the then Electronics Commission of India, sponsored a 3 year project to NAL for the development of a laboratory scale process for hydrothermal synthesis of acicular ferromagnetic - magnetic tape grade chromium dioxide powders for magnetic recording applications. CrO_2 is the only ferromagnetic oxide in the Cr-O system (whose pressure-temperature phase diagram is given in Figure 1). CrO_2 is a non-naturally occurring oxide that could be synthesised as a metastable phase under hydrothermal conditions (simultaneous application of temperature and pressure) and quenched subsequently to room temperature. It is fairly stable, provided a protective layer is formed on its surface to protect it against slow hydrolysis by moisture in air.

Table I. Properties of NAL developed CrO_2 powders in comparison with the Du Pont's CrO_2 powder (International quality)

Property of powder	Du Pont's CrO_2 powders and application areas			NAL's CrO_2 powder
	Audio	Video	Computer	
Coercivity (Oe)	485 - 540	470 - 650	470 - 650	500 -700
Saturation moment (emu/g)	70 -75	65 - 75	65 - 75	70 - 77
Remanant moment (emu/g)	30 -35	30 -35	30 - 35	30 - 34
Moisture % max.	0.5 - 0.7	0.4 - 0.7	0.4 - 0.7	0.5 - 0.7
Tap density (g/cm^3)	0.8 - 1.0	0.8 - 1.0	0.8 - 1.0	0.8 - 1.0
pH at 25°C	3.4 - 3.6	3.4 - 3.6	3.4 - 3.6	3.3 - 3.5
Particle length (μm)	0.4 - 0.5	0.3 - 0.4	0.3 - 0.4	0.3 - 0.6
Specific gravity	4.8 - 4.9	4.8 - 4.9	4.8 - 4.9	4.8 - 4.9
Specific surface area (m^2/g)	24 - 30	25 - 35	25 - 35	25 - 34

Table II. Product phases (major, minor) obtained at different temperatures and at different percentage fills of autoclave

Temperature, °C	Product phases present			
	30% volume fill		60% volume fill	
	Major	Minor	Major	Minor
300	AlOOH		AlOOH	
350	AlOOH	α-Al_2O_3	AlOOH	
375	AlOOH	α-Al_2O_3	AlOOH	
400	α-Al_2O_3	AlOOH	AlOOH	
425	α-Al_2O_3	AlOOH	AlOOH	α-Al_2O_3
450	α-Al_2O_3	AlOOH	α-Al_2O_3	AlOOH
550	α-Al_2O_3		α-Al_2O_3	AlOOH

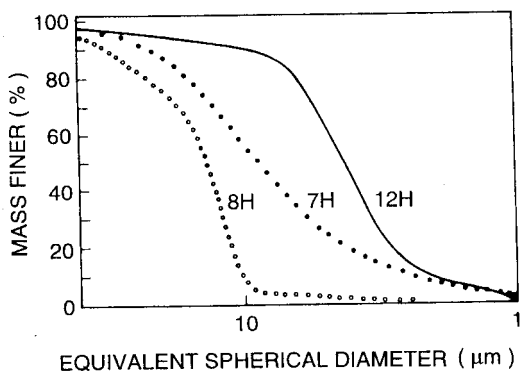

Fig. 6(a). Cumulative particle size distribution graphs of products obtained from the hydrothermal reaction of aluminium metal with 30% volume of fill of the autoclave at 300C (8H), 425C (7H) and 550C (12H)

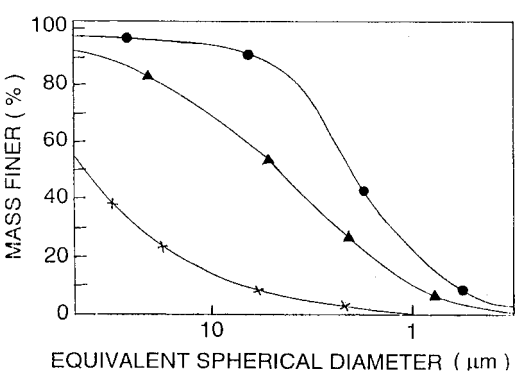

Fig. 6(b). Cumulative particle size distribution graphs of products obtained from the hydrothermal reaction of aluminimum metal with 60% volume of fill of the autoclave at 300C (X), 425C (▲) and 550C (●)

A laboratory process based on hydrothermal decomposition of an aqueous chromium trioxide slurry at 300-350°C and 7-100 MPa pressure in special autoclaves (Figure 2) was developed initially. This process was scaled from 100 g per batch to 5 Kg per batch level. The process flow sheet is given in Figure 3. Simultaneously the physico-chemical and magnetic characterisation (See Figure 4) of the acicular product (Figure 5) was also carried out. The brand of product produced was equivalent to or better than the

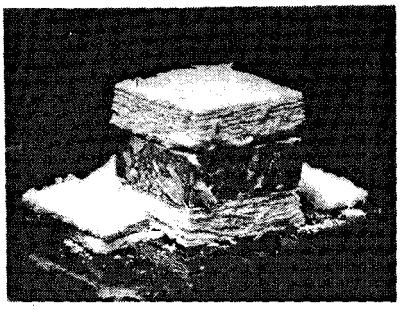

Fig. 7. Typical hydrothermally reacted layered product of alumina

chromium dioxide powder internationally marketed by the only two manufacturers M/s du-Pont, U.S.A. and M/s BASF, Germany (Table I). The studies have been well documented in the form of patents, journal publications, conference presentations and internal reports[1-13].

Hydrothermal decomposition of aluminium metal stock yields ultra fine grade boehmite (β-AlOOH), alumina or alumina - boehmite mixtures in various proportions depending on

Table III. Typical results of doping α-Al_2O_3 powders with manganese, chromium and magnesium

Temp. of reaction (°C/4h)	Wt. of Al taken (g)	% of dopant added (elements)	% Volume of fill	Final pressure (MPa)	Product phases		% Dopant in the final product (elemental)
					Major	Minor	
Cr doped α-alumina (dopant used CrO_3 = 1.00 g)							
340	10.20	5.2	30	35	A	-	5.0(*)
Mn doped α–Alumina (dopant used $MnCo_3$ = 1.36 g reacted with CH_3COOH)							
550	5.50	12	30	65	A	-	5.9(*)
Mg containing alumina (dopant used : (i) Al-5% Mg alloy, (ii) Al - 10% Mg alloy and (iii) Al + magnesium formate = 16.5g)							
550	20.03	5	30	65	A	Sp	15(●)
550	5.40	10	30	65	A	Sp	32(●)
550	5.60	60	36	75	A	Sp	5(●)

A = α-alumina, Sp = Magnesium aluminate $MgAl_2O_4$, * By SEM-EDAX method, ● = By XRD quantitative analysis

the percentage of fill of water (used in the autoclave), temperature and time of hydrothermal reaction. As could be expected, larger quantities of water made the boehmite phase more stable and the on set of its conversion to α-alumina formation was shifted to higher temperatures. Products generated with 30% volume of fill were richer in alumina and much coarser while those generated with 60% volume of fill were finer and richer in β-boehmite as could be seen from Table II and Figure 6 (a & b). These reaction products were uncontaminated with free metal unlike in the case of earlier reactions reported using very fine powders of aluminium. The reaction could be terminated at any stage to generate the products which form as several compact multiple layers all round the metal bar stock. The core bar stock could be separated and used again for further reactions. A typical picture of the product with the residual bar stock after a typical reaction is shown in Figure 7.

The results have been published and Patented[14-19]. The reaction has been extended to obtain alumina powders containing Cr, Mn and Mg as dopants[20] and some typical results are presented in Table III. Further work on hydrothermal synthesis of ultrafine submicron powders of Alumina, Zirconia, Zirconia toughened alumina etc is under progress. Presently a combination of sol-gel synthesis and hydrothermal modification routes is being investigated to obtain these oxide powders in sub-micron sizes.

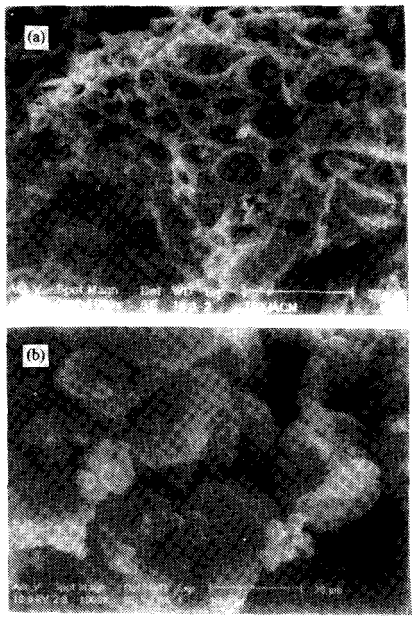

Fig. 8. SEM micrographs of (a) activated charcoal and (b) carbon black used in the experiment

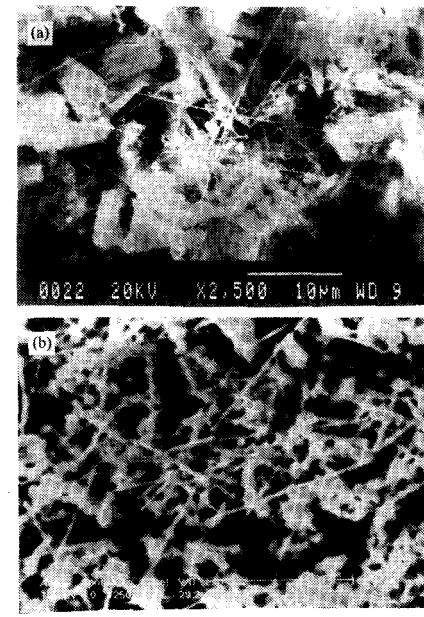

Fig. 9. SEM micrographs of products obtained with (a) activated charcoal and (b) carbon black

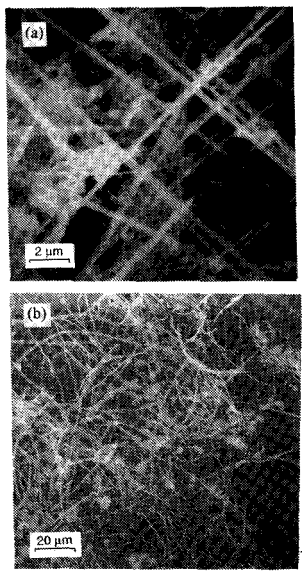

Fig. 10. Representative SEM pictures of products obtained in argon and nitrogen atmospheres at 1700°C from 1 mole of sillimanite (S) and (a) 9.0 moles of carbon black (SCB 90/Argon) (b) 4.5 moles of carbon black (SCB 45/N_2)

3. CARBOTHERMAL REACTIONS

Carbothermal reactions which were first developed for benefication and reduction of oxidic ores have been recently extended for benefication of silicate minerals like clay (Kaolinite in particular) using an inert atmosphere of argon or nitrogen. Cutler et al [21] separated the alumina from the silica part in clay, the silica being reduced to β-silicon carbide. The reactions were catalysed by use of ferric, cobaltic and nickel salts as catalysts in small amounts. By carrying out this reaction under a nitrogen atmosphere Kaolinite was converted to even β-Sialon. Chakladar et al in Canada [22] Dubois et al [23,24] in France and our group in India under an Indo - French Collaborative Project, started around the same time using carbothermic reactions as possible routes for obtaining biphasic mixtures of oxides (e.g. alumina, zirconia and alumina + zirconia) and β-silicon carbide whiskers from aluminosilicate and zircon raw minerals. The minerals are cheap sources to generate the oxide + SiC whisker mixture in - situ rather than by external mixing of the oxides and the expensive silicon carbide whiskers separately.

Table IV. Physical properties of hot pressed composite specimens made from different precursors

Precursor composition	Reaction condition	Final product composition	%SiC in sample (Theoretical)	Density ($g.cm^{-3}$)	Total porosity (%)	% Theoretical density
——Powder——				——Hot pressed body——		
Kaolin + carbon	1750°C N_2/1h	α-Al_2O_3 + SiC(w) + mullite (traces)	44.0	3.23	0.15	84.0
Sillimanite + carbon	1750°C Ar/1h	α-Al_2O_3 + SiC(w)	28.2	3.56	0.03	96
Zircon + carbon	1750°C N_2/1h	m-ZrO_2 + SiC(w)	24.5	4.45	0.02	90.0

Extensive studies on the in-situ Carbothermal reduction of Kaolinite, Sillimanite and Zircon using activated charcoal and carbon black as carbon sources have been carried out under both argon and nitrogen atmospheres. The products obtained were subjected to XRD and SEM studies to delineate the phases formed.

The ratio of carbon black or activated charcoal to the mineral was varied at 3 levels (4.5:1, 5.5:1 and 9.0:1 respectively) and four temperatures of reaction (1550°C, 1600°C, 1650°C and 1700°C respectively) were chosen for different periods of time of reaction in order to study the kinetic evolution of the product phases. An interesting point that has emerged from these studies is that fine and long whiskers of β-silicon carbide are formed at temperatures of 1650°C and the reaction goes to completion at or beyond 1650°C. Addition of ferric and cobalt oxides as dopants also enhanced the SiC whisker formation. Thus in the case of alumino silicate minerals like kaolinite[25] and silimanite[26] the reactions under argon atmosphere proceed via formation of an intermediate mullitic phase and free silica. These convert subsequently to a mixture of alumina and β-silicon carbide whiskers. The very different morphology of activated charcoal and carbon black (Figure.8) were found to affect the reaction rates and the nature of whiskers which were obtained. The reaction rates were generally higher in cases where activated charcoal was used but the formation of -silicon carbide whiskers were vastly superior in the case of carbon black. The peculiar morphology of activated charcoal prevented formation of uniform long and denser whisker growth. Carbon black being in fine powder form promoted free whisker growth in the case of kaolinite and silliminite precursors (Figures 9 & 10). Higher mole ratios of carbon, addition of catalysts, pelletisation of reactants and longer reaction times accelerated as well as completed the reaction in all cases. Under a nitrogen atmosphere when the reactions were carried out under similar conditions β-Sialons and β-SiC were formed[26]. The whiskers formed in this case were not as uniform and as straight as those obtained under argon atmosphere (see Figure 10).

Zircon was also subjected to the same conditions of reaction (activated charcoal and carbon black used, with the same mole ratios of 4.5:1, 5.5:1 and 1.0:1 and reacted at 1550, 1600, 1650 and 1700°C for 1 hour, use of catalysts of ferric, Cobaltic oxides etc.) both in argon and nitrogen atmospheres[27]. In this case a mixture of m-ZrO_2 (with very minor amounts of t-ZrO_2 in the case of nitrogen reactions) and β-silicon carbide whiskers is obtained in all cases. The conversion is complete under argon atmosphere at 1700°C while it does not go to completion even at 1700°C in the case of nitrogen environment. It is found in this case also, that the reaction rate with activated charcoal is higher due to its

Table V. Mechanical properties of hot pressed composite specimens made from different precursors

Precursor composition	Reaction condition	Final product composition	%SiC in sample (Theoretical)	Young's modulus E (GPa)	Fracture strength σ_f (MPa)	Fracture toughness (MPa√)
——————Powder——————				-----Hot pressed body——		
Kaolin + carbon	1750°C N_2/1h	α-Al_2O_3 + SiC(w) + mullite (traces)	44.0	220 230	100 112	5.10 4.85
Sillimanite + carbon	1750°C Ar/1h	α-Al_2O_3 + SiC(w)	28.2	200 208	220 216	8.75 8.67
Zircon + carbon	1750°C N_2/1h	m-ZrO_2 + SiC(w)	24.5	200 204	250 244	7.03 7.04

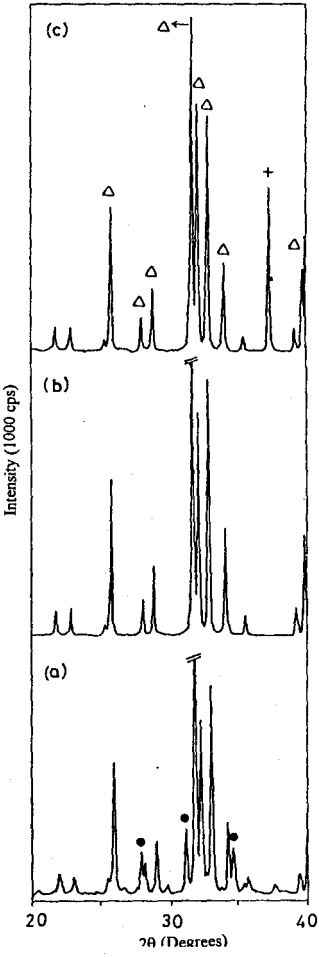

Fig. 11. XRD spectra of TCP + $Ca(OH)_2$ mixture in the molar ratio of (a) 3:1.5 (b) 3:2 and 3:3 (c) 3:4 heat treated to 1000°C for 8h; (●) β-TCP, (Δ) HA, (+) CaO.

higher surface area and it does not give rise to uniform whisker formation, while carbon black produces good, long and uniform whiskers.

Some of the Al_2O_3 + SiC (w) and ZrO_2-SiC (w) composite powder batches prepared by carbothermic reaction from kaolinite, sillimanite and zircon were further hot pressed at 1750°C and 40 MPa pressure in Graphite dies in argon atmosphere to obtain dense composite discs of 30mm diameter x 6mm thickness. Test specimens (bars, 30x6x4 mm^3) were cut from this disc & polished down to 1 μm finish in stages. The products physical as well as mechanical properties (e.g. density, apparent porosity, Young's Modulus, Fracture strength, fracture toughness etc.) have been studied at room temperature. The results are presented in Tables IV & V. The samples derived from sillimanite and zircon possessed good fracture toughness whereas those from kaolin were inferior. This could be probably attributed to the impurities present in kaolinite as compared to the other two minerals.

Studies on the carbothermal reduction of a mixture of aluminosilicate + zircon precursor combination is now being pursued and it has given some interesting preliminary results. A typical reaction product mixture containing α-Al_2O_3, t-ZrO_2 + m-ZrO_2 and β-SiC is obtained in this case. Further studies are in progress.

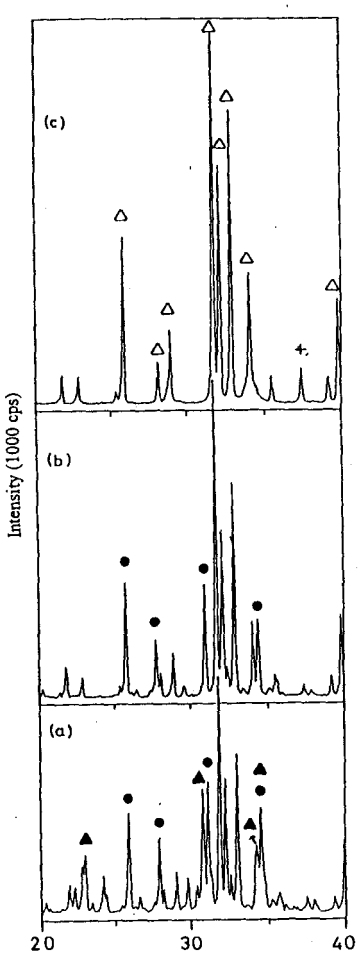

Fig. 12. XRD spectra of TCP + $Ca(OH)_2$ mixture in the molar ratio of (a) 3:1 (b) 3:1.5 (c) 3:3 heat treated to 1250°C for 2h; (●) β-TCP, (▲) α-TCP, (Δ) HA, (+) CaO.

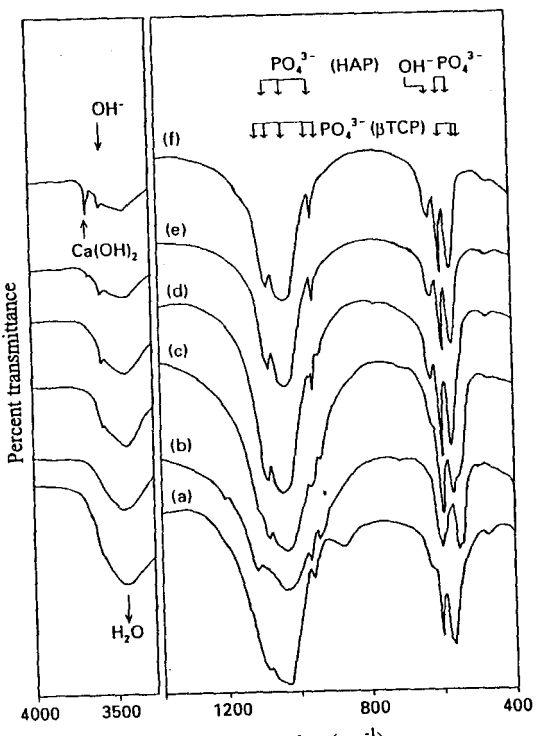

Fig. 13. Infrared spectra of (a) as-received TCP powder and of products obtained from TCP + $Ca(OH)_2$ mixtures (in different molar ratios) on heat treatment at 1000°C for 8h; (b) 3:0; (c) 3:1; (d) 3:1.5; (e) 3:2; (f) 3:3 and 3:4.

4. SOLID STATE REACTIONS FOR SYNTHESIS OF HYDROXYAPATITE AND OXIDE MODIFIED HYDROXYAPATITES FOR BIOCERAMIC APPLICATIONS

Hydroxyapatite (HA) is a ceramic which is present in human and animal bones and tissues and hence called a bioceramic. For all bone replacements, bone joining and also major bone loss in the body due to accidents, it is necessary to have a stock of hydroxyapatite powder. Commercially this powder is quite expensive and hence indigenous processes for synthesis and optimisation of its properties is necessary. In view of the similarity of the microstructure of this bioceramic to that of other ceramic materials being studied (namely ceramics with small porosities at the grain boundaries) a study has been undertaken on the synthesis of HA powder and its sintering to dense products.

The hydroxyapatite has been synthesised by solid state reaction between the commercial calcium phosphate (Laboratory grade, Calcium phosphate tribasic of M/s Robert Johnson, India) and calcium hydroxide (M/s Ranbaxy, India). The precursors were mixed in the molar ratios of 3:0, 3:1, 3:1.5, 3:2, 3:3 and 3:4 into a slurry, slip cast in plaster moulds and heat treated in temperature range of 600°C-1250°C. XRD (Figures 11 & 12) and IR

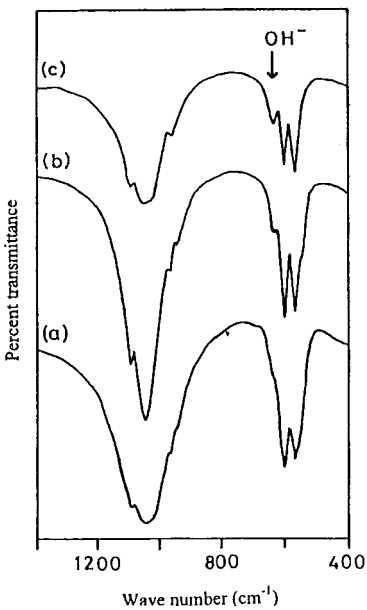

Fig. 14. Infrared spectra of TCP + $Ca(OH)_2$ mixtures in different molar ratios (a)3:1; (b) 3:1.5; (c) 3:2 heat treated to 1250°C for 2h.

spectral characterisation (Figures 13 & 14) of the products of heat treatment (designated T_0, T_1, $T_{1..5}$, T_2, T_3 & T_4) was done. Reaction of 3:2 and 3:3 molar ratio precursors generated pure hydroxyapatite, while those of 3:1 and 3:1.5 ratio reacted products give a mixture of β-tricalcium phosphate (β-TCP) and hydroxyapatite (HA). Reaction of 3:4 molar ratio gave a mixture of HA and free CaO. Products of heat treatment at 1150 and 1250°C while not differing from that of T_0 (β-TCP) and T_2 (HA), those of T_1, $T_{1.5}$, T_3 and T_4 contained products with lesser percentages of HA containing β-TCP (T_1 and $T_{1.5}$) or HA containing CaO (T_3 & T_4) as secondary phases[29,30]. A number of other minor phases are also formed at temperatures lower than 1000°C. The results are summarised in Table VI. The product powders when uniaxially compacted and sintered at 1300°C for 2h yielded sintered bodies with 90-93% of theoretical density of HA. The products had grain sizes in the range of 2-10 μm and pore diameters of 1-2 μm as shown in Figure 15. The XRD & IR spectra of the sintered products are identical to the powders heat treated at 1250°C[31]. Addition of upto 30 wt% of α-Al_2O_3 and m-ZrO_2 powders to the T_2 mixture followed by heat treatment at 1000°C/8h has been attempted. The product was uniaxially compacted and sintered at 1300°C to a material which is β-TCP rich and HA poor. Other phases like t-ZrO_2, $CaAl_2O_4$, $CaZrO_3$ etc. were also present which led to a decrease in density of the final products due to their different sinterabilities[32].

Further Studies on processing of hydroxyapatite powder material by colloidal dispersion followed by its slip casting, sintering as well as evaluation of mechanical properties of sintered product would be presented in the next section.

5. PREPARATION OF OPTIMISED CERAMIC SLIPS AND SLURRIES OF SILICON, SLICON CARBIDE, SILICON NITRIDE AND THEIR MIXTURES FOR SLIP CASTING AND SINTERING OR REACTION NITRIDING.

A wet solution processing route has been practiced for traditional ceramic product development for more than a century. The procedure has been followed by the whiteware and sanitary ware industries. The starting point of the processing is the blending of the major constituent of fine clay powder and its admixtures in required proportions in aqueous media as a slurry with sufficiently high solid loading (60-80 wt% or 55-75 vol % of solids). The industrial practice requires that this wet slurry, called also as slip, consists of homogeneously distributed elementary solid particles, free from agglomeration, in the suspension with a long storage life. This slip is cast into plaster of paris moulds to generate shapes of desired sizes of a component. Subsequent heat treatment of cast and dried component called variously as firing or sintering is required for consolidation into a single object.

The constituents of traditional ceramic ware and pottery are silicate minerals which are predominently ionic and exhibit plastic flow behaviour in their wet state (slip or slurry),

Table VI. Different crystallographic phases analysed[5] by X-ray diffraction method for TCP + $Ca(OH)_2$ combinations after heat treatments at various temperatures / time cycles

Thermal treatment	Heat treated products evolved from β-TCP and $Ca(OH)_2$ mixtures*					
Temperature /Time (^oC/h)	3:0 (T0)	3:1 (T1)	3:1.5 (T15)	3:2 (T2)	3:3 (T3)	3:4 (T4)
80/12	HA DCP DCPD	HA DCP DCPD	-	HA DCP DCPD CH	HA DCP DCPD CH	-
600/8	HA β-TCP β-CPP	HA β-TCP β-CPP DCPD	-	HA β-CPP DCPD CaO	HA β-TCP β-CPP DCPD CH	-
700/8	β-TCP HA β-CPP	HA β-TCP β-CPP	-	HA β-TCP β-CPP	HA β-TCP β-CPP CaO	-
800/8	β-TCP(93) HA(7)	HA(50) β-TCP(50)	-	HA(90) β-TCP(6) CaO(4)	HA(94) β-TCP(6)	-
1000/8	β-TCP(100)	HA(54) β-TCP(46)	HA(84) β-TCP(16)	HA(100)	HA(100)	HA(70) CaO(30)
1150/2	β-TCP(100)	HA(54) β-TCP(46)	-	HA(100)	HA(100)	-
1250/2	β-TCP(100)	HA(49) β-TCP(26) α-TCP(25)	HA(74) b-TCP(26)	HA(100)	HA(90) CaO(10)	-

Starting composition are presented in molar ratios (TCP : $Ca(OH)_2$) as designated below (T_0 - T_4).

$Crystallographic phases analysed: HA = $Ca_{10}(PO_4)_6(OH)_2$, DCP = $CaHPO_4$, DCPD = $CaHPO_4.2H_2O$, CH = $Ca(OH)_2$, β-TCP = β-$Ca_3(PO_4)_2$, β-CPP = β-$Ca_2P_2O_7$, α-TCP = α-$Ca_3(PO_4)_2$

inspite of the high content of solids in them. Their individual particles which develop charged surfaces are kept in a state of suspension making use of the principle of inter-particulate repulsion by electrostatic, steric or electrosteric mechanisms using certain additives called as dispersing agents. Addition of dispersing agents aids to overcome the natural forces of attraction called as van der Waals forces of attraction due to their fine size/ large surface area. Very often these dispersion aids are electrolytes (which are water soluble), easily ionisable salts of either anionic or cationic type or could be just charged long chain polymers with neutral or charged ionic groups appended to their chain. These agents bring into play steric or electrosteric forces to keep the main ceramic powder particles separate and in constant suspension. Their addition, reduces the viscosity of the ceramic blend so that further solid loading is possible to a maximum level. Higher solid loadings yield homogeneously packed solid body with the highest green density for eventually achieving a highly dense object possessing good strength and toughness. The presence of non homogeneous or agglomerated areas (or pockets) due to improper conditioning during the stages of slip formation or slip casting

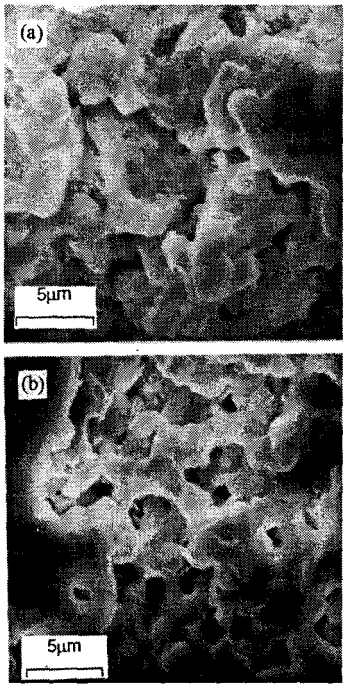

Fig. 15. Typical SEM micrographs of sintered products derived from (a) HA + TCP (T_1) - SHT1 and (b) HA (T_2) - SHT2

give rise to defects and inhomogeneous density distribution in the green stage. These get translated into differential shrinkages and cracking of the slip cast ware on firing or sintering.

Clay bodies with their large surface charges are most suited for wet processing or conditioning. However, the present day advanced ceramic materials are mostly covalently bonded non oxide ceramic materials. e.g. carbides, nitrides and borides of metals e.g. silicon carbide, silicon nitride, boron carbide, aluminium nitride, titanium nitride, titanium carbide, sialons etc. The dispersion of these materials in aqueous media as a homogeneous suspension or slip poses more challenges due to their non plastic behaviour and require pH adjustments or addition of appropriate dispersion aids to create their stable suspensions in water. The assessment of the condition or state of dispersion of these powders in the slip is therefore very important. Some diagnostic tools exist for the assessment of the slips and these are given below.

(i) Sedimentation behaviour in as - prepared condition or by changing the pH of the slip by addition of acids (HCl, HNO_3, acetic acid etc.) or alkalis (NH_4OH, NaOH, alkyl ammonium hydroxides etc.). The measurement of sedimentation height of a slip on standing as a function of pH[2-12] is a simple but powerful diagnostic tool and a pH wherein the particles have a minimum sedimented height is the condition of best dispersion and hence the slip could be optimised by the simple adjustment of pH.

(ii) Measurement of flow characteristics (shear stress developed as a function of rate of shearing) of the slip. The relation is linear (Newtonian) upto a certain solid loading but beyond which thixotropic or dialatent behaviours set in. The slip could therefore be conditioned by assessing the flow (rheological) behaviour by generating the flow curves for different solid loadings and optimising for the near Newtonian behaviour at the highest solid loading. Addition of dispersion aids alter the flow behaviour and aid retention of Newtonian behaviour even at much higher solid loading of slips.

(iii) Determination of viscosity of slips (stress/ shear rate) as a function of shear rate is also a very important measure of the state of dispersion of the solids. Agglomerated slurries have high viscosities while stable non agglomerated slurries have much lower viscosities. Thus, measurement of viscosity of the slip as a function of pH and as a function of solid loading would enable one to determine the optimum slip condition. Optimised slips would also have constant viscosities over a wide range of rotational shear rates rendering a study of viscosity variation versus shear rates a powerful diagnostic tool for assessing the slip condition.

(iv) Measurement of zeta potential of the slip as a function of pH is also used as a diagnostic tool for assessing and optimising the condition of the slips for the best dispersion. Best dispersed condition of the slip is often signalled by a high zeta potential (expressed in ± mv).

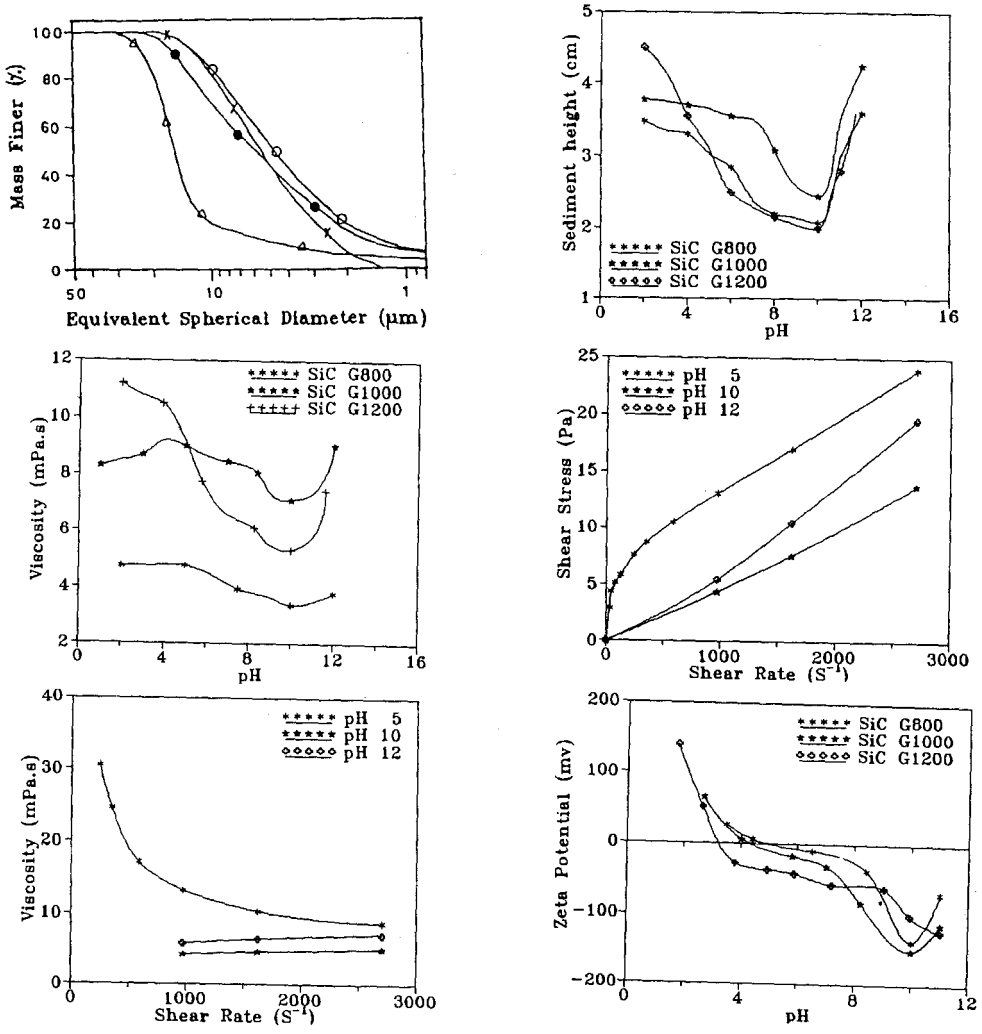

Fig. 16. (a). Effect of pH on particle size distribution of silicon carbide G 1000/2, Δ= pH 3, ● = pH 5, O = pH 10, X = pH 11.5; (b). Sedimentation height (24h) plotted as a function of pH for silicon carbide powders. (c). Viscosity of silicon carbide slips as a function of pH. (d). Shear rate versus shear stress flow curves for silicon carbide (G1200/2) slurry as a function of pH; (e). Viscosity versus shear rate flow curves for silicon carbide (G1200/2) slurry as a function of pH. (f). Zeta potential for silicon carbide slurry as a function of pH.

(v) Information regarding particle size distribution (p.s.d) of particles in a reasonably diluted slip (5 wt%) maintained at different pH values is also a very important tool which compliments the results of the above four diagnostic tools. Thus p.s.d of the slips as a function of pH generates a family of pH-p.s.d. curves in which the best optimised pH generates a curve that is most shifted to the lowest particle size distribution end.

Combining all the above five criteria which are complimentary to each other it is possible to derive the conditions of optimal dispersion of highly solid loaded slips for slip casting followed by sintering, reaction nitriding / reactive bonding etc. of the slip cast body. Thus, lowest sedimentation height, linear Newtonian flow (shear stress vs. shear rate) behaviour, constant lowest viscosity over a range of shear rates, highest zeta potential and the shift of p.s.d to the lowest size end, all occuring at one or more pH conditions (pH windows) would be the combined criteria for optimisation or conditioning of ceramic

Table VII. Various phase formed during nitridation of silicon slip cast bars and silicon powder

Sample nitrided	Nitridation cycle temp./time (^{o}C/h)	Amount of various phases present in the sample (XRD analysis)	Weight gain by XRD (%)	Weight gain by experiment (%)
Slip cast bar Surface (A)	1370/6+ 1400/3+ 1450/1+ 1500/1	α-Si_3N_4 25% β-Si_3N_4 15% β-SiC 50% Si_2N_2O 10%	15 9 23 4 Total 51	48
Core (B)	in Static N_2 (0.18 MPa) in graphite furnace	α-Si_3N_4 37% β-Si_3N_4 23% β-SiC 22% Si_2N_2O 18%	23 14 10 8 Total 55	48
Silicon powder	1400/1 in Static N_2 (018 MPa) in graphite furnace	α-Si_3N_4 68% β-Si_3N_4 19% β-SiC 13%	45 12 6 Total 63	56

Table VIII. Characteristics of green and nitrided compacts of slip cast Si + SiC compositions

Sample identity	Initial Si content (%)	Green density (%)	Nitridation w.r.t. Si (%)	Si_3N_4 formed (%)	Free Si in the product (%)	Bulk density (g/cm^3)	Apparent porosity (%)	M.O.R (MPa)
15NBSC	15	60.9	81.2	18.8	2.6	2.011	34.0	53
25NBSC	25	62.2	78.2	28.8	4.8	2.089	30.3	76
33MBC	33	58.3	76.2	36.2	6.8	1.978	31.7	69
50NBSC	50	58.9	70.3	47.4	12.1	2.015	30.1	85

slips of a single ceramic material. For composite powder mixtures containing more than one powder the optimisation conditions for each has to be determined and judiciously manipulated to get the best additive effects of dispersion.

The above five criteria have been extensively utilised in the laboratory for preparation of optimally dispersed high solid loaded slips of silicon carbide[33] silicon nitride[34] silicon[35] and silicon+silicon carbide mixtures[36] as well as of hydroxyapatite[37]. Results obtained for the optimal dispersion of silicon carbide powders are presented in Figure 16 (a-f) as an illustrative case. It would be seen that a pH=10 and a solid loading of 52 wt% is required for a Newtonian flow behaviour of silicon carbide slips. On the other hand silicon slips have two regions of stability at pH=4-5 and pH=8 and they can be optimally solid loaded (for Newtonian flow behaviour) upto 55 wt%. For silicon nitride, the pH of optimum dispersion was determined to be 10.

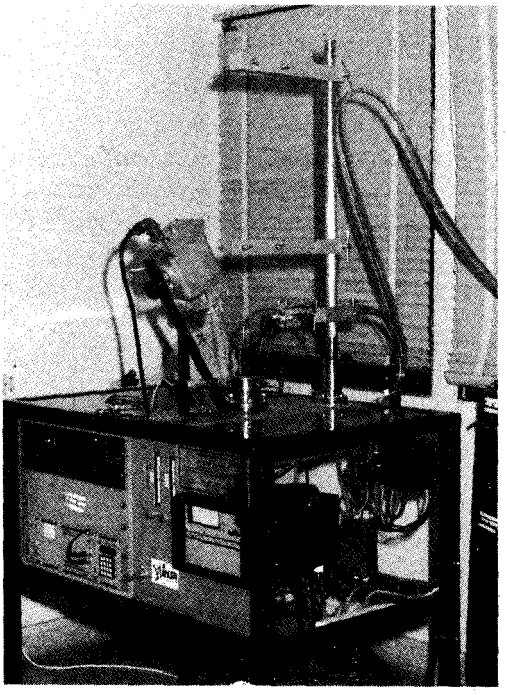

Fig. 17(a). General view of the thermal fatigue machine

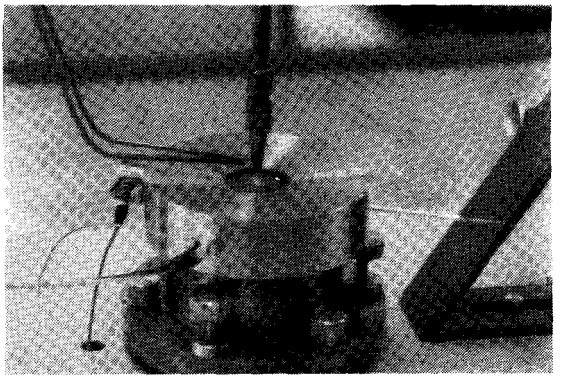

Fig. 17(b). Particular view showing the sample holder surrounded with special wave guide supporting the acoustic emission sensor and the gas torch above.

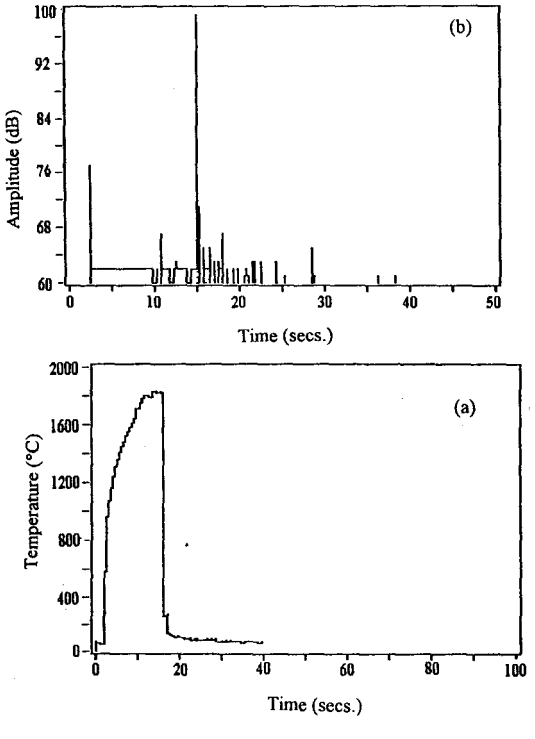

Fig. 18. (a) The temperature versus time graph recorded by pyrometer and (b) AE signals for silicon nitride sample (SN20).

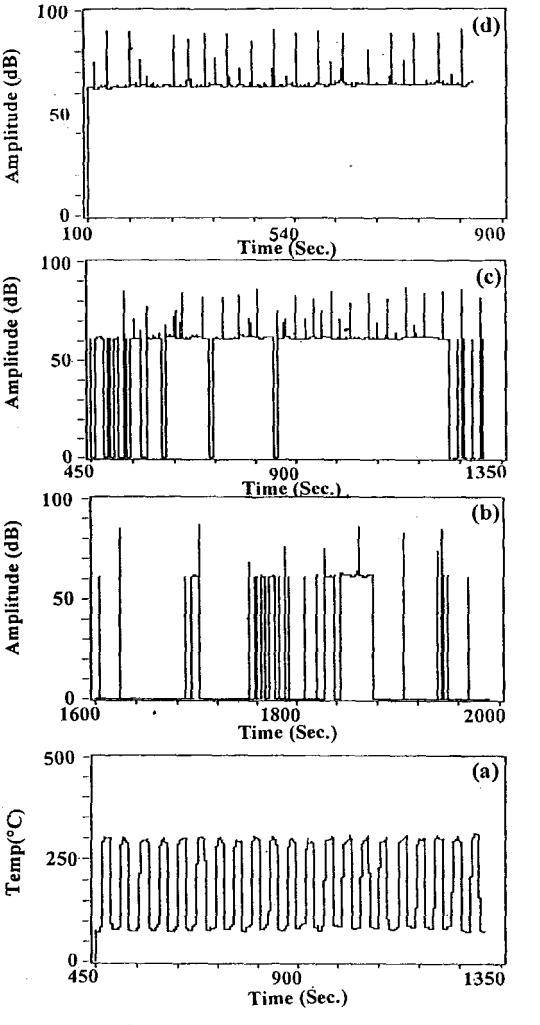

Fig. 19. (a) Typical thermal fatigue cycles and (b-d) evolution of AE with increase in number of cycles (from b to d) showing continuous AE at higher cycles (due to micro-crack growth).

6. SLIP CASTING OF SILICON AND SILICON + SILICON CARBIDE POWDER MIXTURES FOR REACTION NITRIDATION

The optimised slips of silicon and silicon + silicon carbide mixtures with the solid loadings in the range of 60-70 wt% were slip cast in plaster molds. The green bodies thus generated were reaction nitrided in a graphite furnace with graphite felt insultation under 0.18 MPa of static nitrogen gas pressure inside the closed chamber in the temperature range of 1370-1500°C sequentially for periods totalling 12 h. The results for nitridation of pure silicon are presented in Table VII. The high carbon activity of the furnace has resulted in formation of considerable amounts of silicon carbide (50%) on the surface which decreases (22%) as we go into the core of the sample[38]. In the case of silicon + silicon carbide mixture, the slips were cast and nitrided at 1450°C for a total period of 10 h. The nitrided samples were characterised and their mechanical strengths measured on bars (50x9x9 mm) using a 3 point bend fixture (40mm span, 0.5mm min^{-1}) in an Instron 6025 machine. The results obtained are summarised in Table VIII [36].

7. ASCENDING THERMAL SHOCK AND THERMAL FATIGUE TESTING OF CERAMIC MATERIALS

For use in aerospace wherein high temperatures and thermal gradients of large magnitude are encountered, ceramic materials become an obvious choice. However for their use as structural members these materials have to be evaluated for their thermal shock and thermal fatigue behaviour. A novel thermal shock-cum- thermal fatigue test equipment based on the combined use of oxy-hydrogen flame as a heat source (to simulate the fast rate of heating) and a massive water - cooled copper block as the cold surface for applying (on a sample placed across them) a temperature gradient of 2000°C + in less than a minute has been developed. The unit in conjunction with an acoustic emission monitor predicts the onset of cracking in real time. Real time hot spot temperature data acquisition is achieved by using an IR pyrometer mounted oblique to the flame torch while the real time radial peripheral temperature is measured with a fast response thermocouple. The whole system is integrated and run by a PC for on - line data acquisition and display. This unit has been used to screen materials like Al_2O_3, SiC, Si_3N_4, Cordierite (discs and honey combs) etc. for their thermal shock and thermal fatigue behaviour. It is been possible to observe and record the temperature at which the specimens undergo thermal shock failure as well as the microcrack formations during thermal fatigue testing in the case of alumina samples (Figure. 17) in the form of discs of 30mm dia x 2-6 mm thickness. The results are under publication elsewhere[39-42]. Modellisation of the data using a finite Element soft ware to obtain temperature and thermal stress distribution patterns of the samples undergoing the tests are in progress. It is now possible to completely study the thermal shock and thermal fatigue behaviour of ceramic specimens at high temperature (Figures 18 & 19) on this novel test equipment developed as a part of Indo-French collaborative project.

8. CONCLUSION

Some results from work done in the area of ceramic material synthesis, ceramic processing, slip casting, reaction nitriding, mechanical testing and fabrication and use of an ascending thermal shock-cum-thermal fatigue test unit for characterisation of ceramic materials are described.

ACKNOWLEDGEMENTS

The authors thank Prof. S. Ramaseshan, Dr. A. K. Singh, Dr. S. R. Valluri, Prof. R. Narasimha, Dr. K. N. Raju and Dr. T. S. Prahlad who have greatly encouraged and provided the facilities for carrying out the reported work. The authors are thankful to Prof. Fantozzi, Dr. J. Dubois and Dr. C. Olagnon of INSA de Lyon for the help in the thermal shock - thermal fatigue test equipment. The authors are thankful to Dr. S. Usha Devi, C. Balasingh and Dr. Kalyani Vijayan for XRD studies, Mr. M. A. Venkataswamy, Dr. T. A. Bhaskaran and Dr. R. V. Krishnan for SEM studies and Dr. A Giridhar and Dr. Sudha Mahadevan for IR studies. The authors also thank Electronics Commission of India and Indo-French Centre for Promotion of Advanced Research, New Delhi, for financial support to some of the work reported herein.

REFERENCES

1. Jaleel, V. A., Aswath, C., and Kannan, T. S., Magnetic Society of India Transactions (MSI transactions), 1980, **4**, 18.
2. Jaleel, V. A., Aswath, C., Bhaskar, T. A., Sivaraman, R. and Kannan,T. S., The 13th Annual Conference of Electron Microscopy Society of India, Bangalore, February 1981.
3. Jaleel, V. A. and Kannan, T. S., Bull. Mater. Sci., 1983, **5**, 231.
4. Kannan, T. S. and Jaleel, V. A., The 7th Tech. Meeting of Magnetics Society of India, Bangalore, 1983.
5. Kannan, T. S. and Saravana, B. V., TM-Engg-2-79, January 1980.
6. Kannan, T. S., Jaleel, V. A., Cheluvaraju, A. and Saravana, B. V., Report NAL.-PD-8536 (1985).
7. Jaleel, V. A., Ranjan, M., and Kannan, T. S., The ICF-V Conference, Bombay 1989.
8. Jaleel, V. A., Ranjan, M. and Kannan, T. S., in: Advances in Ferrites - Proc. of the ICF-V Conference, Bombay, Eds., C.M. Srivastava and M.J. Patni, 1989, p.115.
9. Sarvana, B. V. and Kannan, T. S., PD-ES-8601 (1986).
10. Project Document MT- 8536 presented as completion/final report to the Electronics Commission, Dec. 1985.
11. Kannan, T. S., Jaleel, V. A. and Aswath, C., Patent no. 627/Del/87 (refiled in December 1990).
12. Kannan, T. S., Jaleel, V. A., Cheluvaraju, A., and Sarvana, B. V., Patent no. 882/Del/87 (refiled in December 1990)
13. Kannan, T. S., "Preparation of chromium dioxide for magnetic recording applciations" in : Advances in High Pressure Science and Technology, Ed., A.K. Singh, Tata McGraw-Hill, New Delhi, 1996, pp. 237-247.
14. Yoshimura, M., Kikugawa, S., and Somiya, S., in : "High Pressure in Research and Industry", Proc. of the 8th AIRAPT Conference and 19th EHPRG onference, Eds., C.M. Backman, T. Johan and L. Tegner , Sweden, August 1981, p. 793.
15. Toraya, H., Yoshimura, M., and Somiya, S., J. Amer. Ceram. Soc., 1982, **65,** C-172.

16. Idem, ibid ,1983, **66,** 148.

17. Kannan, T. S., Panda, P. K. and Jaleel, V. A., Patent No. 440/DEL/95, March 1995.

18. Panda, P. K., Jaleel, V. A., Usha Devi, S., and Kannan, T. S., in: "Advances in High Pressure Science and Technology", Ed., A.K. Singh, Tata McGraw Hill, New Delhi, 1995, p. 249.

19. Kannan, T. S., Panda, P. K. and Jaleel, V. A., J. Mat. Sci. Lett., 1997, **16**, 830.

20. Kannan, T. S., Panda, P. K. and Jaleel, V. A., Trans. Ind. Ceram. Soc.,1999, **58**, 1.

21. Bechtold, B. C. and Cutler, I. B., J. Am. Ceram. Soc., 1980, **63**, 271.

22. Chaklader, A. C. D., Das Gupta, S., Lin, E. C. Y., Gutowski, B., J. Am. Ceram. Soc., 1992, **75**, 2283.

23. Dubois, J., Murat, M., Carbonneau, X., Gardon, R., Appl. Clay Science, 1995, **10,** 187.

24. Dubois, J., Murat, M., Amroune, A., Carbonneau, X., Gardon, R., and Kannan, T. S., Appl. Clay. Science., 1998, **13,** 1.

25. Panda, P. K., Mariappan, L. and Kannan, T. S., Ceram. Int., 1999, **25,** 467.

26. Panda, P. K., Mariappan, L., Jaleel, V. A., Kannan, T. S., Dubois, J. and Fantozzi, G., J. Mater. Chem., 1996, **6**, 1395.

27. Panda, P. K., Mariappan, L., Jaleel, V. A., Kannan, T. S., Amroune, A., Dubois, J. and Fantozzi, G., J. Mater. Sci., 1996, **31,** 4277.

28. Jaleel, V. A., Panda, P. K. and Kannan, T. S., in: Proc - Composite Materials of COMPEAT - 1998, Eds. R.R. Bhat, S. Ghosh and C.S. Sivaramakrishnan, Pub. NML, Jemshedpur, 1998, pp. 160.

29. Ramachandra Rao, R., Roopa, H. N., Kannan, T. S. and Rao, K. J., Metals Materials and Processes, 1996, **8**, 309.

30. Ramachandra Rao, R., Roopa, H. N. and Kannan, T. S., J. Mater. Sci. Mater. in Medicine, 1997, **8**, 511.

31. Ramachandra Rao, R., Roopa, H. N., and Kannan, T. S., Trans. Indian. Ceram. Soc., 1998, **57**, 73.

32. Ramachandra Rao, R. and Kannan, T. S., Trans. Indian Ceram. Soc., 1999, **58**, 64.

33. Ramachandra Rao, R., Roopa, H. N. and Kannan, T. S., Ceram. Int., 1999, **25**, 223.

34. Ramachandra Rao, R., Roopa, H. N. and Kannan, T. S., Trans. Indian Ceram. Soc., 1999, **58**, 25.

35. Ramchandra Rao, R., Roopa, H. N. and Kannan, T. S., J. Eur. Ceram. Soc., 1999,**19**, 2763.

36. Ramachandra Rao, R., Roopa, H. N. and Kannan, T. S., J. Eur. Ceram. Soc., 1999, **19**, 2145.

37. Ramachandra Rao, R. and Kannan, T. S., Paper accepted for publication in: J. Am. Ceram. Soc., (March 2000).

38. Ramachandra Rao, R., Roopa, H. N. and Kannan, T. S., J. Mat. Sci. Letters., 1996, **15**, 1956.

39. P. K. Panda, Ph.D. Thesis, Etude de L'endommagement de Materiaux Ceramiques Par choc Thermique Ascendant; Compartment a La Fatigue Thermique et modellisation, INSA de Lyon, France,1999.

40. Kannan, T. S., Panda, P. K., Singh, A. K., Dubois, J., Olagnon, C. and Fantozzi, G., PDMT 9901, Oct. 1999.

41. Madusoodana, C. D., Das, R. N., Umarji, A., Panda, P. K. and Kannan, T. S., SIAT '99, 1999 (Paper : 990008), 161.

42. Panda, P. K., Mariappan, L., Kannan, T. S., Dubois, J., Olagnon, C., Ascending thermal shock-cum-thermal fatigue test equipment and thermal shock and thermal fatigue behaviour of ceramic materials: Pts I-III submitted to J. Am. Ceram. Soc., for publication.